ELSEVIER

Polymer 42 (2001) 5389–5399

polymer

www.elsevier.nl/locate/polymer

Blends of single-site linear and branched polyethylene. I. Thermal characterisation

B.S. Tanem[a,*], A. Stori[b]

[a]NTNU, Department of Machine Design and Materials Technology, Norwegian University of Science and Technology, Rich. Birkelands vei 2b, Trondheim, Norway

[b]SINTEF Materials Technology, Department of Polymer and Composites, Forskningsveien 1, Postboks 124 Blindern, N-0314 Oslo, Norway

Received 2 August 2000; accepted 24 November 2000

Abstract

Blends of a low-molecular-weight linear polyethylene and several different ethylene–hexene copolymers are investigated using differential scanning calorimetry and transmission electron microscopy. All blend components are based on single-site catalysts. For cooling rates higher than 1°C/min, reorganisation effects are generally present, making the interpretation of the blends less clear. The reorganisation effects are found to be dependent of the amount of comonomer in the branched blend component, the compositions of the blends and the cooling and heating rates applied. For a low content of the linear blend component, even 1.8 mol% comonomer content in the branched blend component is sufficient to create two crystal populations during crystallisation. For higher amounts of the linear blend component 2.5 mol% comonomer will result in two crystal populations.

Keywords: Polyethylene blends; Cocrystallisation; Single-site materials

1. Introduction

Blends of linear and branched polyethylene have received much attention during the last decades. The possibility to enhance material properties and the need to get a deeper understanding of the underlying morphology has triggered this development. The development of single-site catalysts represented an important step in this manner. Single-site materials are believed to have a well-defined structure [1,2] making them ideal as blends components in a morphology study of blends. However, limited work has been presented on polyethylene blends involving single-site materials [3–7]. Zhao et al. [3] report cocrystallisation for all blend compositions in blends of linear polyethylene (LPE) and a single-site ethylene–octene copolymer containing 0.72 mol% short chain branches (SCB). By increasing the comonomer content in the branched component to 1.4 mol%, cocrystallisation is found to occur when the LPE content in the blends is higher than 50%. Finally, increasing the comonomer content to 4.8 mol%, no cocrystallisation is observed. Therefore, Zhao et al. [3] conclude that the maximum amount of comonomer allowed in the branched component still observing cocrystallisation, probably is much lower in blends with single-site materials, than in blends involving Ziegler–Natta materials. Lee et al. [4] have studied blends of LPE and a single-site ethylene–butene copolymer containing 3.4 mol% comonomer. Cocrystallisation was only found to occur when the amount of the branched component was less than 20% (by weight).

We were originally interested in the morphology of blends of a low-molecular weight LPE and higher molecular weight ethylene–hexene copolymers, where both blend components are based on single-site technology. Such blends with a bimodal molecular weight distribution have become important in plastic industry today. However, the thermal behaviour of these blends turned out to be more complex than expected and it is crucial to be able to understand the development of the observed morphology. Thermal behaviour of blends of a low molecular weight LPE and eight different ethylene–hexene copolymers are presented in this work. The blends are studied with differential scanning calorimetry (DSC). In a continuation of this work, the blends and blend components used here are examined by optical microscopy, atomic force microscopy and transmission electron microscopy. The results from the latter three techniques will be presented in a separate paper [8]. Only a few TEM pictures will be shown here to clarify the discussion.

* Corresponding author. Fax: +47-73-59-41-29.

E-mail addresses: bjorn.s.tanem@immtek.ntnu.no (B.S. Tanem), aage.stori@matek.sintek.no (A. Stori).

0032-3861/01/$ - see front matter
PII: S0032-3861(00)00872-7

Table 1
Characterisation of the single-site materials used in this work

	M_w[a]	M_w/M_n[a]	T_m[b]	T_c[c]	Com[d]	Density[e]
LPE	26,000	5	132.9	121.0	–	> 970.0
LLDPE(1)	90,000	2.7	123.9	112.7	1.0	937.4
LLDPE(2)	150,000	2.2	119.0	107.6	1.7	925.1
LLDPE(3)	115,000	2.5	117.9	106.9	1.8	927.8
LLDPE(4)	62,000	3.3	115.5	105.3	2.5	928.5
LLDPE(5)	105,000	2.3	110.9	98.9	4.2	919.6
LLDPE(6)	85,000	2.2	103.0	88.9	5.7	902.3
LLDPE(7)	58,000	10	95.5	83.4	7.5	902.8
LLDPE(8)	34,000	5	71.5	60.2	–	–

[a] Weight-averaged molecular weight (M_w) and polydispersity (M_w/M_n) determined from GPC.
[b] Melting point in °C as observed in DSC using a heating rate of 10°C/min after a cooling rate of 1°C/min.
[c] Crystallisation temperature in °C as observed in DSC using a cooling rate of 1°C/min.
[d] Mol% butyl branches determined from NMR and FTIR.
[e] kg/m^3 determined from gradient column.

2. Experimental

2.1. The materials

The materials used throughout this study include an LPE and eight different ethylene–hexene copolymers, denoted LLDPE(i), $i = 1.8$. Relevant information of each sample is listed in Table 1. The amount of comonomer in the samples is found to be in the range from 1.0 mol% to beyond 8 mol%. Unfortunately, the weight-average molecular weights of the samples differ to some extent. The polydispersity index is low for the samples except LLDPE(7), which has a low-molecular weight fraction. A narrow distribution of molecular weights will probably eliminate any effect of molecular segregation in the samples during crystallisation. The molecular weight of the linear blend component is significantly lower than the copolymers, giving the resulting blends a bimodal character. The molecular weights and the polydispersities of the samples were determined from GPC, as described elsewhere [9]. LLDPE(i) $i = 1.5$ are experimental qualities made at NTNU in Trondheim. LLDPE(6) and LLDPE(7) are qualities obtained by solvent extraction from a bimodal sample kindly supplied from Borealis AS as an experimental quality. A description of the extraction technique is found in Ref. [9]. LLDPE(6) represents the extracted fraction obtained using hexane as the solvent, LLDPE(7) represents the fraction obtained using heptane as the solvent, while LLDPE(8) represents the fraction obtained using pentane as the solvent. Blends of the LPE component and each of the LLDPE(i) $i = 1.8$ components were made in various proportions in solution as described in Refs. [7,9]. A blend containing x% (by weight) of LPE and y% (by weight) of LLDPE(i) will be denoted x/y LPE/LLDPE(i). As an example, 10/90 LPE/LLDPE(1) means a blend consisting of 10% (by weight) of LPE and 90% (by weight) of LLDPE(1). Film was prepared using a Schwabenthan polystat 200T press operating at 160°C by allowing the material to melt in the press, followed by a pressure sequence of a few seconds. The samples were then taken out from the press and cooled down to room temperature in air.

2.2. Nuclear magnetic spectroscopy (NMR)

The amount of butyl branches for three of the samples was evaluated from ^{13}C NMR spectra obtained using a Bruker Avance DPX 400. Polymer powder (40–50 mg) was taken in an NMR-tube and 0.2 ml deuterated benzene and 0.5 ml 1,2-dichlorbenzene were added. The NMR-tube was thereafter evacuated and placed in an oven at 120°C for 2 h, allowing the polymer to be dissolved in the solvent. The spectra were recorded at 400 MHz and 120°C. The acquisition time was 2 s, the delay time 7 s and the number of scans were 6000. The chemical shifts were assigned to the different sequences according to Hsieh et al. [10].

2.3. Fourier-transformed infrared spectroscopy (FTIR)

The powder of each sample was pressed into a film under the same conditions as described above. The film thickness was 0.3 mm. The spectra were recorded on a Bruker-IFS66V spectrophotometer equipped with a DTGS-detector. The nominal resolution was 2 cm^{-1}. Two hundred scans were taken. In order to quantitatively assign the number of butyl branches from FTIR, a calibration curve (calibrated against NMR results) was obtained, using the 893 cm^{-1} band. This band has been assigned to a methyl rocking mode for branches larger than ethyl [11]. Fourier deconvolution and combined Lorentz–Gauss curve fitting were necessary to obtain quantitative data. It turned out to be difficult to obtain proper film from the LLDPE(8) component. The amount of comonomer in this sample is therefore judged to be over 8 mol%, based on results obtained from the other samples.

2.4. Density

Circular disks of approximately 5 mg were put in DSC sample pans. After a scan to erase effects of thermal history, the samples were heated to 170°C at 10°C/min and cooled to 10°C at a cooling rate of 1°C/min. The samples were then taken out of the DSC sample pans and allowed to sink in Davenport gradient columns containing different ratios of

water and isopropylalcohol. The samples were kept in the gradient columns for 10 min before the density values were recorded. The values given in Table 1 represent the average value of three parallels.

2.5. DSC

Thermal examination of the blends was performed with a Perkin–Elmer DSC-7 flushed with nitrogen and equipped with a water-cooling unit. Identical circular flat disks of 1.5–2.0 mg, being approximately 100 μm in thickness were encapsulated in DSC sample pans. This will probably eliminate any differences among the samples due to thermal lag during the heating scan [12]. The DSC sample pans were equipped with holes allowing the remaining xylene to be effectively transported away by the inert nitrogen atmosphere during the first heating scan in DSC. A small piece of aluminium sheet of 1.5–2.0 mg was placed in the reference pan. This will eliminate the mass difference between the sample and reference, and will give rise to a more stable baseline [12]. The second run was recorded, in order to eliminate the effects of thermal history and the effects of the remaining solvent. The first and second run programs were equal and according to the following scheme: heating from 10 to 170°C applying a heating rate of 10°C/min, keep at 170°C for 5 min, followed by a cooling sequence from 170 to 10°C. The cooling rate was varied, the actual values will be given in the text as they appear. The heating rate was always 10°C/min (except those scans performed to check whether reorganisation/recrystallisation occurred).

Calibration was regularly checked against the onset melting temperature of a pure Indium sample using the same heating rate as employed in the measurements. The baseline was regularly checked using empty sample pans. The melting temperature of the samples was identified with the maximum in the endothermic peak. The enthalpies of fusion were converted to degrees of crystallinity by taking the enthalpy of fusion of a perfect polyethylene crystal as 290 J g^{-1} [13].

2.6. Thermal fractionation

Thermal fractionation was performed on the blend components using a technique involving successive self-nucleation/annealing (SSA), introduced by Müller et al. [14]. This technique represents a method to qualitatively characterise the distribution of SCB in copolymers.

The samples were heated from 30 to 170°C, held for 5 min before cooled down to 30°C. The heating and cooling rate applied was 10°C/min. This was done to erase any effects of thermal history of the samples. The samples were thereafter heated to an annealing temperature where all the crystalline regions except small crystals were melted, e.g. for LLDPE(*i*) this temperature was 124°C. The samples were held for 5 min at this temperature and were thereafter cooled down to 30°C again. The crystals that did not melt at the first annealing temperature self-nucleated the sample during the cooling step. After this step, the samples were reheated to a second annealing temperature, which was 4°C lower than the first annealing temperature, and held for 5 min. At this second annealing temperature parts of the melted crystals will be nucleated by the unmelted crystals and crystallise isothermally, while the unmelted crystals will anneal. The remaining part of the melt will crystallise at the following cooling step down to 30°C. This procedure continues until an annealing temperature of 60°C is reach. Then the samples were heated to 150°C and multiple melting peaks were recorded.

2.7. Transmission electron microscope (TEM)

All the blends discussed in this work are investigated using TEM, but most of these results will be presented in a separate paper [8]. However, TEM pictures of the blends 10/90 LPE/LLDPE(3) and 10/90 LPE/LLDPE(5) will be shown here. Films for TEM were sealed in DSC sample pans and gained the same thermal history as the films for DSC prior to the melting scans, i.e. cooling rates of 1 and 10°C/min were applied. The samples were thereafter treated in chlorsulfonic acid. Our methods of sample preparation follow the method introduced by Kanig [15,16] and are described in detail elsewhere [9]. The blend 10/90 LPE/LLDPE(3) was treated in the acid for eight days, while the blend 10/90 LPE/LLDPE(5) was treated for five days.

3. Results and discussion

3.1. Blend components

DSC melting endotherms of the branched components LLDPE(*i*) $i = 1.7$ used in this study are given in Fig. 1. The cooling rate prior to the shown heating traces was 10°C/min. A systematic decrease in melting point is observed as the amount of comonomer increases, the relationship is approximately linear. This is in agreement to the results obtained by others [17]. The depression in melting

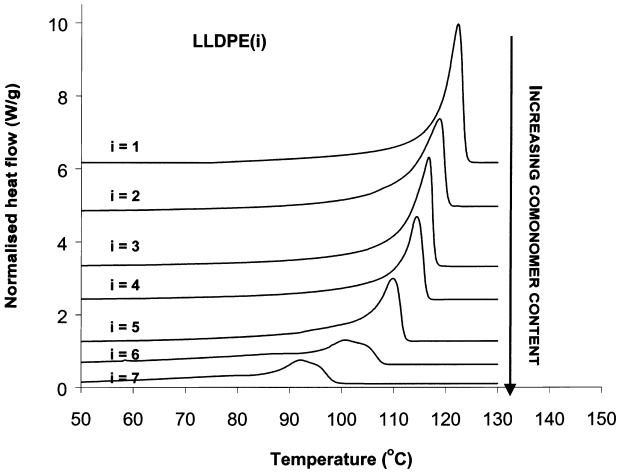

Fig. 1. DSC melting endotherms of the different LLDPE(*i*) $i = 1...7$ used in this study, listed for increasing comonomer content. The cooling and heating rates applied were 10°C/min.

point for increasing comonomer incorporation is explained by the occurrence of shorter ethylene sequences between SCB in samples containing high amounts of comonomer compared to samples containing lower amounts of comonomer. Furthermore, the crystallinity of each sample was calculated using results from density measurements and observed heats of fusion in DSC. The crystallinity calculated from density measurements were somewhat higher than results from DSC, in agreement to earlier published results [17]. The crystallinity in the samples is generally found to decrease as the amount of comonomer increases, e.g. the crystallinity was calculated to 58.3% in LLDPE(1) compared to 32.7% in LLDPE(7) (from density measurements). However, there are variations among the samples, e.g. the crystallinity was found to be higher in LLDPE(4) compared to LLDPE(2), even though the comonomer content is significantly higher in LLDPE(4) compared to LLDPE(2). However, other factors such as the molecular weights of the samples are known to affect the crystallinity [18] of the polymer samples. The variation in molecular weights among the samples used in this work (Table 1) might therefore obscure a systematic variation in the crystallinity, expected from comonomer incorporation.

As mentioned in Section 1, single-site materials are expected to have a more uniform distribution of SCB along the polymer chains compared to Ziegler–Natta based materials. To qualitatively assess the comonomer distribution in the different copolymers used in this work, the samples were fractionated using a thermal fractionation technique based on SSA. This method allows the observations of structural heterogeneity in the branched blend components used in this work, since several fractions are separated by the content of short chain branching. The results obtained from the SSA technique are shown in Fig. 2. Multiple melting peaks are observed in all samples. The samples LLDPE(1) and LLDPE(3) show one prominent "linear" peak together with several smaller peaks, while the other samples show several peaks of more uniform height. The comonomer distribution in the samples is generally dependent of the catalysts employed during polymerisation and the polymerisation conditions [19–22]. For the samples used in this study, different catalysts and polymerisation conditions are employed. The comonomer distributions are therefore expected to vary among the components. A semiquantitative approach has been utilised to compare the homogeneity in short chain distribution among the samples. According to Knox [23], the depression in the heat of fusion of the copolymer is given by the relation

$$\Delta H_f = (63 - 5.5 \times C)\text{cal/g} \quad (1)$$

where C denotes the number of SCB/1000 carbon atoms along the main chains. From this equation and the linear relationship between the melting points of the copolymers used in this study and the amount of comonomer, a relation between the observed heat of fusion and the melting temperature is obtained. The partial areas of each melting peak are calculated and compared to the total area. From the semiquantitative approach described above the amount of material that constitute each of the melting peaks are determined. The results from these calculations indicates that the comonomer distribution is generally more homogeneous in samples containing low amounts of comonomer compared to samples containing higher amounts of comonomer. In LLDPE(3) 76% of the material is found to melt within a temperature interval of 16°C, while this is reduced to 61% in LLDPE(5). However, variations among the samples are observed. It is therefore concluded that the branched blend components used in this work show some structural heterogeneity which increases with increasing comonomer

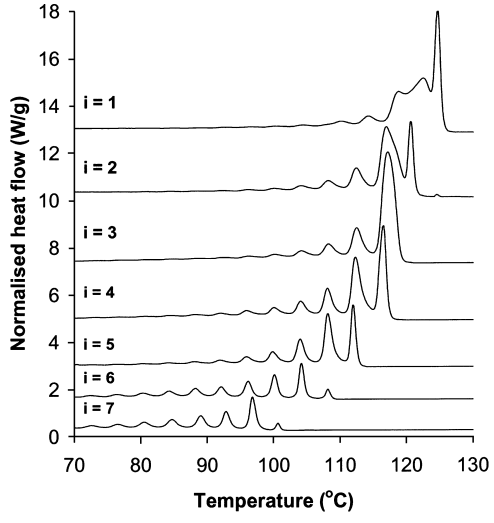

Fig. 2. DSC melting endotherms of the branched blend components LLDPE(i) $i = 1...7$ after thermal fractionation using the SSA-technique. The cooling and heating rates applied were 10°C/min.

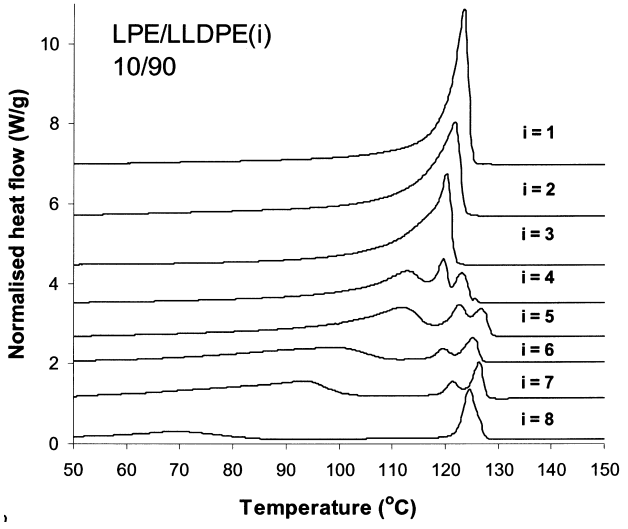

Fig. 3. DSC melting endotherms of the blends 10/90 LPE/LLDPE(1), $i = 1...7$. The heating and cooling rates applied were 10°C/min.

incorporation. Structural heterogeneity has also been observed by others in different single-site materials [14,24,25].

3.2. Blends — "fast" cooling

DSC melting endotherms of the blends 10/90 LPE/LLDPE(i) $i = 1.8$ are shown in Fig. 3. The heating and cooling rates were 10°C/min. The blends 10/90 LPE/LLDPE(i), $i = 1.3$ show apparently only one single melting peak and will be referred to later in the text. Three melting peaks are found in the blend 10/90 LPE/LLDPE(4). The form and position of the low-temperature peak indicates that this peak represents melting of mainly the LLDPE(4) component, i.e. a component rich in LLDPE(4). At higher temperatures additional two melting peaks appear. Similar behaviour is observed in the blends 10/90 LPE/LLDPE(i) $i = 5.7$. In order to explain the origin of these melting peaks the heating rate during the melting scans was varied. Fig. 4 shows the results obtained from the blend 10/90 LPE/LLDPE(7) when the heating rate was varied. The cooling rate prior to the heating scans in Fig. 4 was 10°C/min. It is clear from Fig. 4 that the ratio between the high-temperature peak and the medium-temperature peak changes with the heating rate. The low-temperature peak is apparently unchanged. The medium temperature peak appears to grow at the expense of the high temperature peak as the heating rate is increased. This behaviour is more prominent when the cooling rate prior to melting is varied. This is shown in Fig. 5. The heating rate is now constant, 10°C/min. From Fig. 5 it is clear that the high-temperature peak becomes smaller as the cooling rate is lowered and finally disappears when the cooling rate is low enough, 1°C/min. in this case. The blends 10/90 LPE/LLDPE(i) $i = 4.6$ are found to possess a similar cooling and heating rate dependency.

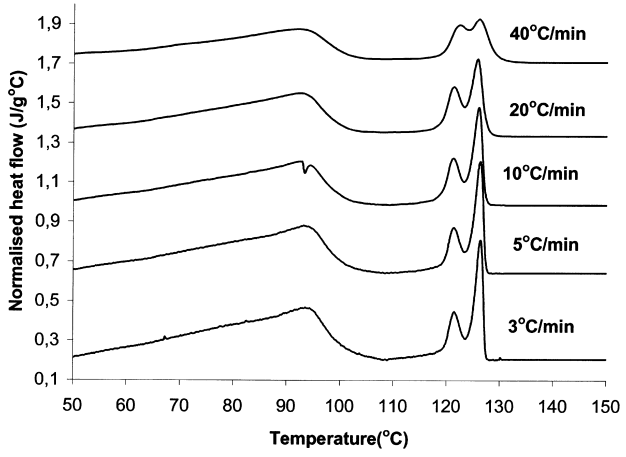

Fig. 4. DSC melting endotherms of the blend 10/90 LPE/LLDPE(7) for different heating rates applied. The cooling rate prior to the melting

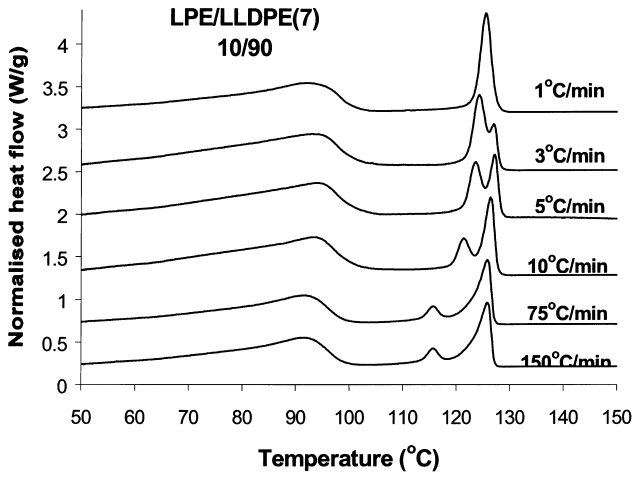

Fig. 5. DSC melting endotherms of the blend 10/90 LPE/LLDPE(7) for different cooling rates applied prior to the melting. The heating rate was 10°C/min.

Such behaviour has been observed and discussed earlier in similar blend systems [7,9] and by others in different blend systems [26–28], and is believed to be explained from reorganisation of less organised material during the melting. However, the systematic increase in comonomer incorporation that is present in the samples employed in this work allows for the observation of a dependency between the reorganisation effects and the amount of comonomer in the branched blend components. In Fig. 2 it is shown that the high temperature peak in the blends 10/90 LPE/LLDPE(i) $i = 4.7$, increases at the expense of the medium temperature peaks as the amount of comonomer in the branched blend component increases. When the amount of comonomer is increased beyond 8 mol% the splitting apparently disappears, as seen in the blend 10/90 LPE/LLDPE(8). Similar behaviour has been observed in rapidly quenched blends of the same LPE component and ethylene–butene copolymers, where the amount of comonomer is above 5.0 mol% [9].

The melting behaviour of the pure branched blend components is quite similar to the results presented in Fig. 1, when the cooling rate is decreased to 1°C/min. The only major difference is that all the components show higher melting points.

3.3. Blends — slow cooling

DSC melting endotherms of the blends 10/90 LPE/LLDPE(i) $i = 1.7$ recorded after applying a cooling rate of 1°C/min are shown in Fig. 6. This low cooling rate was chosen to avoid reorganisation effects, as shown in Fig. 3, where the heating rate was 10°C/min. The blend 10/90 LPE/LLDPE(1) shows a well-defined single melting point, indicating that only one crystal population is present. The observed melting point and crystallisation temperature of the blend 10/90 LPE/LLDPE(1) differ only 0.5% from those calculated using weighted values of the two

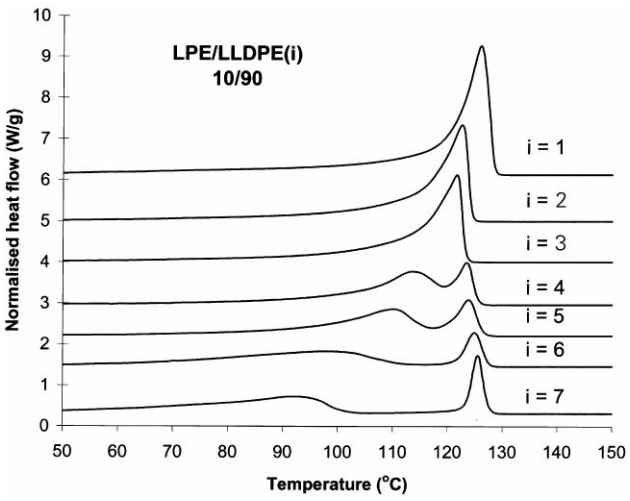

Fig. 6. DSC melting endotherms of the blends 10/90 LPE/LLDPE(i) $i = 1...7$ listed for increasing comonomer content in the LLDPE(i) components. The heating rate applied was 10°C/min. The cooling rate applied was 1°C/min.

components in the blend, indicating cocrystallisation among the blend components. Furthermore, the degree of crystallinity of this blend, based on enthalpy of fusion measurements is lower than the calculated crystallinity based on the assumption that each component form separate crystallites. See Table 2 for details. A low crystallinity of the blend compared to the pure blend components has been taken as an argument in favour of cocrystallisation [2,29]. The observed melting behaviour of the blend 10/90 LPE(LLDPE(1) therefore suggests that cocrystallisation is present to an extensive degree in this blend. The same conclusion can be made when the cooling rate prior to the melting is 10°C/min (Fig. 3). By increasing the amount of comonomer in the branched blend component to 1.8 mol% ($i = 3$) the melting peak of the blend becomes much broader as compared to the pure branched component, and extends far into the low-temperature region. This is observed in the blend 10/90 LPE/LLDPE(3). In this blend the observed melting point and crystallisation temperature are 2.2% higher than those calculated using weighted values of the two blend components, assuming cocrystallisation. However, the calculated crystallinity of the melting peak in 10/90 LPE/LLDPE(3) is lower than the crystallinity calculated assuming separate crystallites. See Table 2 for details. As previously mentioned, this is an argument in favour of cocrystallisation. It is therefore believed that cocrystallisation is present to a certain degree also in this blend. However, the broad melting peak suggests the existence of a second melting peak, indicating that the amount of cocrystallisation is reduced as compared to the blend 10/90 LPE/LLDPE(1). This conclusion is supported from observations in TEM. A TEM picture of the blend 10/90 LPE/LLDPE(3) is shown in Fig. 7. Apparently only one single type of lamellae seems to be present. However, the measurements of a large number of lamellae give a broad distribution of lamellae thickness, with a clear tendency towards a bimodal distribution, which is not present e.g. in the blend 10/90 LPE/LLDPE(1). The results from TEM and DSC therefore indicate that the blend 10/90 LPE/LLDPE(3) contains two major crystal populations. One of the crystal populations is made from a cocrystal of LPE and LLDPE(3) while the second population consists of LLDPE(3)-rich crystals.

The results from thermal fractionation of the LLDPE(3) sample, shown in Fig. 2 might explain the DSC and TEM observations. Thermal fractionation of the LLDPE(3) blend components reveals a dominant "linear" fraction at 116°C, and several minor fractions at lower temperatures. The amount of comonomer in the dominant fraction is probably low enough to enable this fraction to cocrystallise with the LPE blend component during the cooling. The amount of comonomer in the other nearest fractions is probably much higher than present in the large fraction, representing chains that mostly will be excluded from the LPE lamellae during crystallisation and generate a secondary crystal population.

The melting peak of the blend 10/90 LPE/LLDPE(2) is also rather broad and extends into the low-temperature regime. However, the melting peak of the pure LLDPE(2) blend component is also rather broad and TEM pictures of

Table 2
Melting point, crystallisation temperature and crystallinity of the blends 10/90 LPE/LLDPE(i) $i = 1...7$. T_m^1 (T_c^1) denotes the melting temperature (crystallisation temperature) of the high-temperature peak in the blends, T_m^2 (T_c^2) denotes the melting temperature (crystallisation temperature) of the low-temperature peak in the blends. ω_o refers to the observed crystallinity of the high-temperature peak in the blend (ω_o^1) and the low-temperature peak in the blend (ω_o^2). ω_c refers to the calculated crystallinity of the high-temperature peak in the blend (ω_c^1) and the low-temperature peak in the blend (ω_c^2), assuming completely separate crystals. The blends experienced a cooling rate of 1°C/min, and a heating rate of 10°C/min

Blend	T_m		T_c		ω_o		ω_c	
	T_m^1	T_m^2	T_c^1	T_c^2	ω_o^1	ω_o^2	ω_c^1	ω_c^2
LPE/LLDPE(1)	125.5	–	114.3	–	56.9	–	9.1	54.3
LPE/LLDPE(2)	122.5	–	110.9	–	49.3	–	9.1	42.5
LPE/LLDPE(3)	121.7	–	110.9	–	48.6	–	9.1	48.1
LPE/LLDPE(4)	123.5	114.1	113.2	105.6	9.2	31.1	9.1	33.5
LPE/LLDPE(5)	123.9	110.2	112.7	101.7	10.9	31.5	9.1	37.9
LPE/LLDPE(6)	124.9	97.7	116.8	95.4	6.8	27.6	9.1	29.5
LPE/LLDPE(7)	125.5	92.0	115.5	87.4	8.1	20.5	9.1	24.8

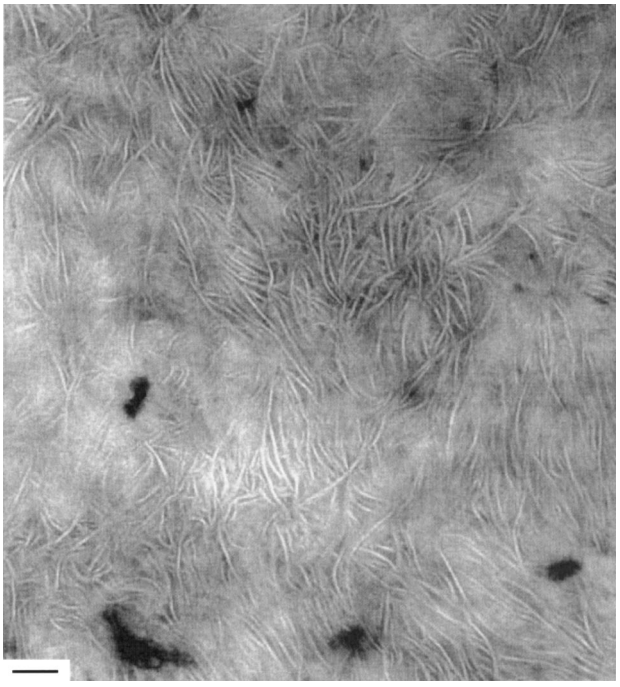

Fig. 7. TEM picture of the blend 10/90 LPE/LLDPE(3). The blend experienced a cooling rate of 1°C/min prior to examination in TEM. The scale bar in the picture is 100 nm.

this blend do not indicate a bimodal distribution of lamella thickness.

The blends 10/90 LPE/LLDPE(2) and 10/90 LPE/LLDPE(3) are found to behave similarly when the cooling rate is 10 and 1°C, shown in Figs. 3 and 6, respectively.

By further increasing the amount of comonomer in the branched blend component to 2.5 mol%, two separate melting peaks are found, as seen in the blend 10/90 LPE/LLDPE(4) in Fig. 6. The DSC results clearly indicate the existence of two separate crystal populations in this blend. The level of crystallinity of the low-temperature peak is, however, found to be lower than that calculated assuming complete segregation of the two components (Table 2). Furthermore, the shape of the low-temperature peak is found to be less sharp than the pure LLDPE(4) component. These observations might partly be explained from the inclusion of some LLDPE(4) chains into the LPE lamellas during crystallisation. In that case, the remaining LLDPE(4) chains in the blend, excluded from the LPE crystals, are expected to have a higher overall degree of branches than the pure LLDPE(4) component and should therefore melt at a lower temperature; and this is, in fact, observed. The low-temperature peak in the 10/90 LPE/LLDPE(4) blend has a melting point 1.1°C lower than observed for the pure LLDPE(4) component.

However, it is also possible that some of the LPE chains are included into the LLDPE(4) lamellas during crystallisation, interfering with the crystalline structure of this component. For this reason, the low-temperature peak is thought to represent melting of a fraction rich in the LLDPE(4) component. Furthermore, it is clear that the melting point of the high-temperature peak in the blend 10/90 LPE/LLDPE(4) is substantially lower (9.4°C) than the melting point of the pure LPE component. Puig et al. [30] have observed a similar depression of the melting point of the high-temperature peak in a blend of an LPE and an LDPE and suggest three reasons for this behaviour:

(a) a diluent effect caused by the LDPE melt;
(b) cocrystallisation of the LDPE component into the LPE lamella;
(c) a lower lamellae thickness of the LPE component in the blend.

Puig et al. [17] find all three mechanisms to contribute, the most important being the last factor. Based on these results, the depression of the high-temperature peak in the blends shown in Fig. 6, most probably have a complex reason and cannot be explained from cocrystallisation alone. However, the issue to be stressed here is that this effect is prominent in the 10/90 LPE/LLDPE(4) blend and could be explained, at least partly, from a limited degree of cocrystallisation among the blend components.

A further increase in the amount of comonomer in the branched component will result in a better separation of the two melting peaks, as seen in the remaining blends: 10/90 LPE/LLDPE(5), 10/90 LPE/LLDPE(6) and LPE/LLDPE(7), shown in Fig. 6. As discussed earlier in this paper, reorganisation and/or recrystallisation effects during the heating scan can result in two separate melting peaks. Therefore, several heating rates were applied (3, 5, 10, 20 and 40°C/min) to the blends 10/90 LPE/LLDPE(i) $i = 4...7$. However, no principal difference was found by varying the heating rate. Based on these observations it is therefore believed that the occurrence of two separate melting peaks found in some of the blends in Fig. 6 represents blends having two separate crystal populations.

These results are supported from TEM. In contrast to the TEM picture of the blend 10/90 LPE/LLDPE(3) shown in Fig. 7, the TEM pictures of the blends 10/90 LPE/LLDPE(i) $i = 5...7$ clearly demonstrate the existence of two separate crystal populations. A TEM picture of the blend 10/90 LPE/LLDPE(5) is shown in Fig. 8. A few relatively long and straight lamellas are found in a matrix of significantly thinner lamellas. The thicker lamellas are believed to represent lamellas rich in the LPE component, while the thinner lamellas are believed to represent LLDPE(5)-rich lamellas. These results are in agreement with the DSC results in Fig. 6.

Some interesting properties of the pure branched components and the blends are shown in Fig. 9. As described earlier in this paper, there seems to exist a linear relationship between the melting points of the pure branched blend components and the amount of comonomer incorporated in these samples. This is shown in Fig. 9. Furthermore, it is clear that the melting points of the LPE-rich peaks in the blends are significantly lower than the melting point of the pure LPE component, in those blends showing two melting

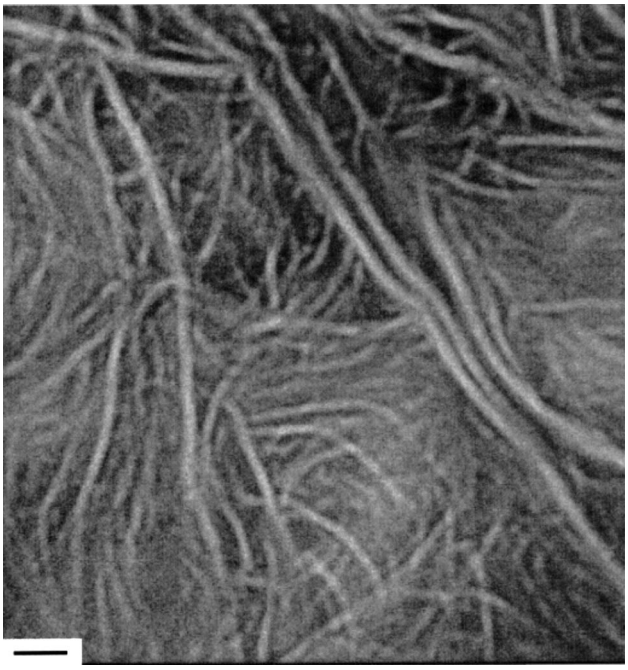

Fig. 8. TEM picture of the blend 10/90 LPE/LLDPE(5). The blend experienced a cooling rate of 1°C/min prior to the examination in TEM. The scale bar in the picture is 30 nm.

peaks in DSC. This observation was discussed above for the blend 10/90 LPE/LLDPE(4), and explained partly from cocrystallisation. However, from Fig. 9 it is clear that a similar depression is also present in the blends 10/90 LPE/LLDPE(5), 10/90 LPE/LLDPE(6) and 10/90 LPE/LLDPE(7). This depression is found to be 6.9°C in the blend 10/90 LPE/LLDPE(7) and increases as the comonomer content in the branched component decreases. This indicates that the branched component has a noticeable influence on the crystallisation of the LPE component in all blends. Furthermore, it is clear from Fig. 9 that the melting points of the LLDPE(*i*)-rich peaks in the blends are significantly lower than the melting points of the corresponding pure LLDPE(*i*) peaks, not only for the 10/90 LPE/LLDPE(4) blend discussed above, but also for all blends showing two melting peaks. This result might indicate that even in e.g. LLDPE(6) there exists chain segments that are able to cocrystallise with LPE, giving the remaining excluded LLDPE(6) chains a higher overall degree of branches melting at lower temperatures. The thermal fractionation of the LLDPE(6) component, shown in Fig. 2, indicate that such chain segments probably are present.

Furthermore, from Table 2 it is clear that the crystallinity of the LLDPE-rich peaks is lower than that calculated assuming separate crystallites, in all blends showing two melting peaks. Based on these results it is concluded that a limited degree of cocrystallisation seems to be present in all blends used in this work.

An apparently perfect cocrystallisation seems to be present in the 10/90 LPE/LLDPE(1) blend, while the blends 10/90 LPE/LLDPE(6) and 10/90 LPE/LLDPE(7) show cocrystallisation only to a limited degree. There does not seem to exist any sharp limit between materials able to cocrystallise and materials unable to cocrystallise, which we would expect when single-site materials are employed. The transition between a single melting point (in 10/90 LPE/LLDPE(3)) and two separate melting points (in 10/90 LPE/LLDPE(4)), shown in Fig. 6, is believed to be an effect due to the limited resolving capability of the DSC instrument. The broad tail of the 10/90LPE/LLDPE(3) blend, extending far into the low-temperature regime suggests that this peak actually consists of two melting peaks close in temperature. This is supported from TEM and the thermal fractionation

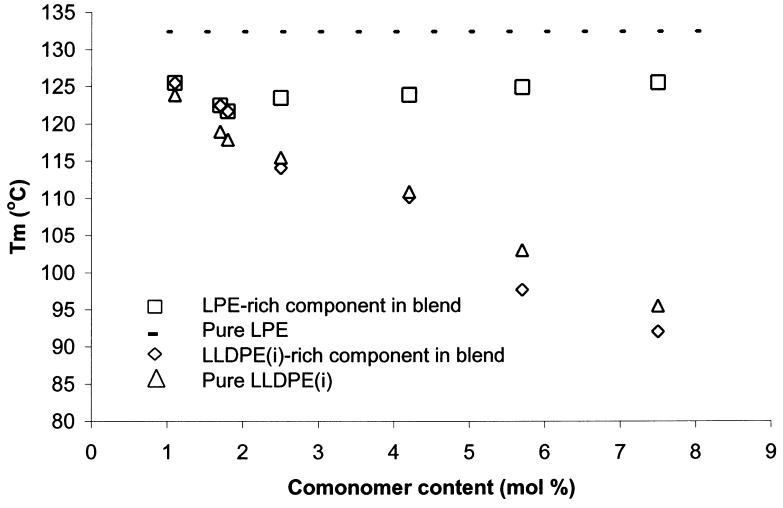

Fig. 9. Details of the blends presented in Fig. 6. The dotted lines indicate the melting point of the pure LPE component (132.9°C). The rectangular boxes indicate the melting points of the LPE-rich components in the blends, for increasing amount of comonomer in the branched blend components. The rotated squares indicate the melting points of the LLDPE-rich components in the blends for increasing amount of comonomer in the branched blend components. The triangles indicate the melting points of the pure branched blend components for increasing amounts of comonomer incorporated.

of the sample. The limited resolving capability of the DSC instrument will, however, result in one single, but broad melting peak. It is convenient to state the resolving limit of the DSC instrument in terms of the amount of comonomer in the branched blend component. For the sample preparation technique, types of material and crystallisation history of the samples used in this study, the DSC resolution limit seems to be approximately 2.0 mol% hexene incorporation in the branched blend component.

3.4. Other blend compositions

The behaviour observed in the blends 10/90 LPE/LLDPE(1) $i = 1...7$ is found to be somewhat different when the ratio of the blend components is varied. DSC melting endotherms of the blends 50/50 LPE/LLDPE(i) $i = 1...7$ are shown in Fig. 10. The cooling rate prior to the heating scans shown in Fig. 10 was 10°C/min. The blends 50/50 LPE/LLDPE(1) and 50/50 LPE/LLDPE(3) show rather sharp well-defined melting peaks indicating the existence of only one crystal population. The melting endotherm of the blend 50/50 LPE/LLDPE(2) indicates the presence of a secondary crystal population. However, the lamella thickness distributions, measured from TEM pictures, showed no bimodal tendency in this sample (or the 50/50 LPE/LLDPE(1) and the 50/50LPE/LLDPE(3) blend samples). It is therefore believed that only one single crystal population is present in these blends. When the amount of comonomer is increased from 1.8 to 2.5 mol%, two separate melting peaks appear, the same observation as for the 10/90 blends. No apparent effect of reorganisation during heating is found to be present in these blends containing 50 wt% of the linear blend component, applying a cooling rate of 10°C/min. However, if the amount of the linear blend component is reduced to 25 wt%, an additional sharp peak

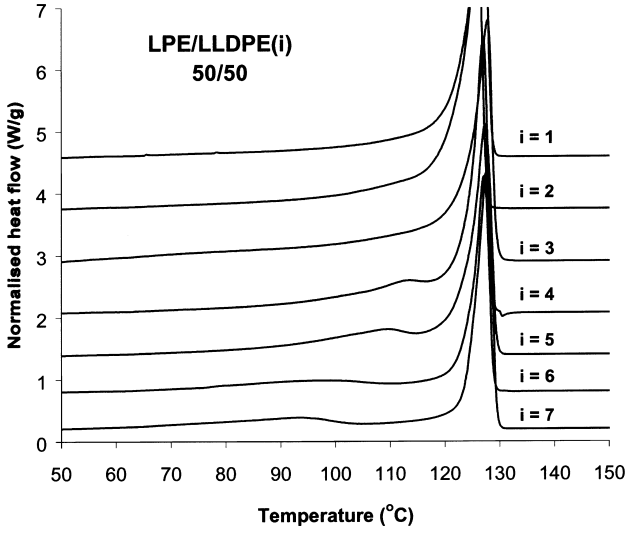

Fig. 10. DSC melting endotherms of the blends 50/50 LPE/LLDPE(i) $i = 1...7$ listed for increasing comonomer content in the LLDPE(i) component. The heating and cooling rate applied was 10°C/min.

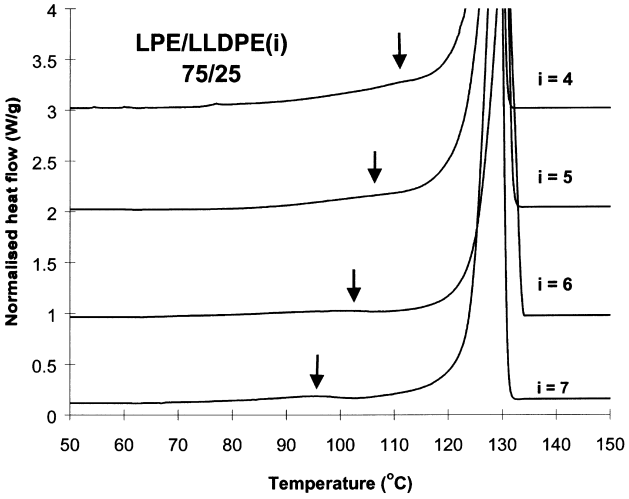

Fig. 11. DSC melting endotherms of the blends 75/25 LPE/LLDPE(i) $i = 1...7$ listed for increasing comonomer content in the LLDPE(i) component. The heating and cooling rate applied was 10°C/min.

is present (not shown here). It has been demonstrated elsewhere that reorganisation effects will also be present in 50/50 blends of similar materials when the cooling rate is increased [9]. When the cooling rate is decreased to 1°C/min, the behaviour of the blends 50/50 LPE/LLDPE(i) $i = 1...7$ are similar to the behaviour presented in Fig. 10.

DSC melting endotherms of the blends 75/25 LPE/LLDPE(i) $i = 4...7$ are shown in Fig. 11. The cooling rate prior to the heating scans shown in Fig. 11 was 10°C/min. As observed for the other blend ratios, two melting peaks are present as the amount of comonomer is increased from 1.8 to 2.5 mol%. The LLDPE(i)-rich peaks in the blends are hardly visible unless the vertical scale is expanded (the LLDPE(i)-rich peaks are indicated by arrows in Fig. 11). The remaining blends 75/25 LPE/LLDPE(i): $i = 1...3$ are not included in Fig. 11, since the minor melting peaks in the blends 75/25 LPE/LLDPE(i) $i = 4...7$ then would be invisible. However, these blends show one sharp melting peak, indicating the existence of a single crystal population. As for the 50/50 blends, no reorganisation effects are found to be present. However, when the cooling rate prior to melting is increased, a shoulder (or sometimes a small and very sharp peak) is visible in addition to the two other melting peaks [9]. The behaviour of the blends shown in Fig. 11 is found to be similar when the cooling rate is reduced to 1°C/min.

3.5. Effects of the phase behaviour in the melt

In an earlier work, the phase behaviour in the melt for similar blend systems was investigated [9]. One of the blend systems used in Ref. [9] was comparable to the blend LPE/LLDPE(5) used here. In Ref. [9] the blends were held in the melt and thereafter quenched, involving extremely high

cooling rates. The blends were thereafter explored by DSC, TEM and AFM, and a morphology map of the melt phase of the blends could then be constructed. A morphology map of the blend system in Ref. [9], comparable to the blend system LPE/LLDPE(5) is given in Fig. 12. The morphology map is simply a coordinate system, where the x-axis gives the amount (in wt%) of the linear component in the blend. The y-axis gives the temperature from which the melt was quenched. A particular blend, quenched from a particular temperature determines a coordinate (x,y) in the morphology map. This coordinate (x,y) will be written as an "M" in the morphology map if the DSC and TEM results indicate that this particular blend is believed to be homogeneous (mixed) in the melt prior to quenching. The letter "S" will be used to indicate that the blend is believed to be separated in the melt prior to quenching. As shown in Fig. 12, the 10/90 blend is found to be phase separated in the melt at the whole temperature region from 130 to 200°C, and expected to persist further down in temperature. It is therefore expected that crystallisation of the 10/90 LPE/LLDPE(5) took place from a phase separated melt, in agreement to the observation of two crystal population in the blend 10/90 LPE/LLDPE(5) from DSC and TEM in Figs. 6 and 8, respectively. The same conclusion can be made for blends of LPE/LLDPE(5) containing 50% (by weight) of the LPE component (Fig. 12). However, if the amount of the linear component is increased to 75% (by weight) the morphology map in Fig. 12 indicates that the melt is found to be homogeneous in the whole temperature region from 130 to 200°C, and expected to persist for lower temperatures. It is therefore believed that crystallisation of the 75/25 LPE/LLDPE(5) blend took place from a homogeneous melt. The observation of two separate crystal populations in this blend from DSC (Fig. 11) and from TEM (not shown here) therefore indicates that this separation of the blend components is a crystallisation induced separation. The other blends in this study differ somewhat from the blends used in Ref. [9], and will not be discussed here further.

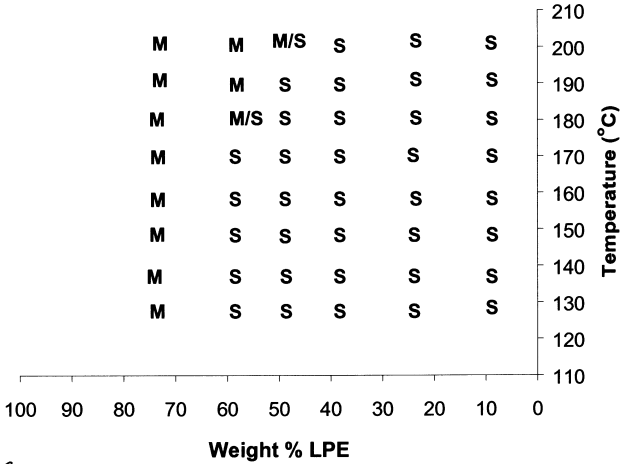

Fig. 12. Morphology map of a blend system similar to the LPE/LLDPE(5) blend system. The letter "S" is used to indicate that the blend is believed to be separated in the melt, for a given composition of the blend and at a given temperature. The letter "M" is used to indicate that the blend is believed to be homogeneous (mixed) in the melt.

4. Conclusions

In this work a low-molecular-weight single-site LPE has been blended with several different single-site ethylene–hexene copolymers. The blends experienced two different cooling rates, 10 and 1°C/min, and were examined by DSC and TEM. Based on the experimental procedures that are employed in this work, the most important finding are listed below:

- In blends containing 10 wt% of the linear blend component, even 1.8 mol% comonomer in the branched blend component is sufficient to create two separate crystal populations. This limit is lower than observed in blends containing Ziegler–Natta based materials, indicating a more homogeneous distribution of SCB in the single-site materials used here. However, a limited degree of cocrystallisation seems to be present even for relatively high amount of comonomer in these blends. This is most probably the result of some structural heterogeneity in the branched blend components. In blends containing 50 and 75 wt% of the linear blend component, 2.5 mol% comonomer in the branched blend component is sufficient to create separate crystal populations.
- Reorganisation effects are found to depend on the cooling and heating rates applied, the composition of the blends and the amount of comonomer in the branched blend components.
- The branched blend components show considerable structural heterogeneity in the comonomer distribution, even though the materials are synthesised using single-site catalysts. The comonomer distribution seems to be more heterogeneous when more comonomer is incorporated, in the branched blend components used in this work.

Acknowledgements

Financial support from the Norwegian Research Council (NFR) under the Polymer Science Program is gratefully acknowledged. The authors also want to thank Heidi Nornes Bryntesen at Borealis for GPC measurements and Irene Helland at Borealis for help with density characterisation of materials.

References

[1] Brintzinger HH, Fischer D, Mulhaupt R, Rieger B, Waymouth RM. Angew Chem, Int Ed Engl 1995;34:1143.

[2] Mandelkern L, Alamo RG, Wignall GD, Stehling FC. TRIP 1996;4(11):377.
[3] Zhao Y, Liu S, Yang D. Macromol Chem Phys 1997;198:1427.
[4] Lee SY, Jho JY, Huh W. J Ind Engng Chem 1998;4(3):258–62.
[5] Rana D, Lee CH, Cho K, Lee BH, Choe S. J Appl Polym Sci 1998;49:2441.
[6] Rana D, Cho K, Woo T, Lee BH, Choe S. J Appl Polym Sci 1999;74:1169.
[7] Tanem BS, Stori Aa. Thermochim Acta 2000;345:73.
[8] Tanem BS, Stori Aa. Submitted for publication.
[9] Tanem BS, Stori Aa. In preparation.
[10] Hsieh ET, Randall JC. Macromolecules 1982;15:1402.
[11] Blitz JP, McFaddin DC. J Appl Polym Sci 1994;51:13.
[12] Behrstein VA, Egorov VM. In: Kemp TF, Kennedy JF, editors. Differential scanning calorimetry of polymers. Ellis Horwood Series in Polymer Science and Technology, 1994, sections 1 and 5.
[13] Zhou H, Wilkes GS. Polymer 1997;38(23):5735.
[14] Müller AJ, Hernández ZH, Arnal MJ, Sánchez JJ. Polym Bull 1997;39:654.
[15] Kanig G. Kolloid Z Z Polym 1973;251:782.
[16] Kanig G. Prog Colloid Polym Sci 1975;57:176.
[17] Alamo RG, Mandelkern L. Thermochim Acta 1994;238:155.
[18] Alamo RG, Chan EKM, Mandelkern L, Voigt-Martin IG. Macromolecules 1992;25:6381.
[19] Bruni C, Pracella M, Masi F, Menconi F, Ciardelli F. Polym Int 1994;33:279.
[20] Sinclair KB. Plast Engng 1994;50:19.
[21] Starck P. Polym Int 1996;40:11.
[22] Kim YS, Chung CI, Lai SY, Hyun KS. J Appl Polym Sci 1996;59:125.
[23] Knox JR. J Polym Sci C 1967;18:69.
[24] Fu Q, Chiu F-C, McCreight KW, Guo M, Tseng WW, Cheng SZD, Keating MY, Hsieh ET, Deslauries PJ. Macromol Sci -Phys B 1997;36(1):41.
[25] Starck P, Lehmus P, Seppälä JV. Polym Engng Sci 1999;39(8):1444.
[26] Paukkeri R, Lehtinen A. Polymer 1993;34(19):4075.
[27] Paukkeri R, Lehtinen A. Polymer 1993;34(19):4083.
[28] Fonesca CA, Harrison IR. Thermochim Acta 1997;313:37.
[29] Wignall GD, Londono JD, Lin JS, Alamo RG, Galante MJ, Mandelkern L. Macromolecules 1995;28:3156.
[30] Puig CC, Hill MJ, Odell JA. Polymer 1993;34:3402.